

Measurement of the Branching Fraction of $\psi(2S) \rightarrow \gamma\pi^0$

M. Ablikim¹, M. N. Achasov^{4,c}, P. Adlarson⁷⁶, O. Afedulidis³, X. C. Ai⁸¹, R. Aliberti³⁵, A. Amoroso^{75A,75C}, Q. An^{72,58,a}, Y. Bai⁵⁷, O. Bakina³⁶, I. Balossino^{29A}, Y. Ban^{46,h}, H.-R. Bao⁶⁴, V. Batozskaya^{1,44}, K. Begzsuren³², N. Berger³⁵, M. Berlowski⁴⁴, M. Bertani^{28A}, D. Bettoni^{29A}, F. Bianchi^{75A,75C}, E. Bianco^{75A,75C}, A. Bortone^{75A,75C}, I. Boyko³⁶, R. A. Briere⁵, A. Brueggemann⁶⁹, H. Cai⁷⁷, X. Cai^{1,58}, A. Calcaterra^{28A}, G. F. Cao^{1,64}, N. Cao^{1,64}, S. A. Cetin^{62A}, X. Y. Chai^{46,h}, J. F. Chang^{1,58}, G. R. Che⁴³, G. Chelkov^{36,b}, C. Chen⁴³, C. H. Chen⁹, Chao Chen⁵⁵, G. Chen¹, H. S. Chen^{1,64}, H. Y. Chen²⁰, M. L. Chen^{1,58,64}, S. J. Chen⁴², S. L. Chen⁴⁵, S. M. Chen⁶¹, T. Chen^{1,64}, X. R. Chen^{31,64}, X. T. Chen^{1,64}, Y. B. Chen^{1,58}, Y. Q. Chen³⁴, Z. J. Chen^{25,i}, Z. Y. Chen^{1,64}, S. K. Choi¹⁰, G. Cibinetto^{29A}, F. Cossio^{75C}, J. J. Cui⁵⁰, H. L. Dai^{1,58}, J. P. Dai⁷⁹, A. Dbeyssi¹⁸, R. E. de Boer³, D. Dedovich³⁶, C. Q. Deng⁷³, Z. Y. Deng¹, A. Denig³⁵, I. Denysenko³⁶, M. Destefanis^{75A,75C}, F. De Mori^{75A,75C}, B. Ding^{67,1}, X. X. Ding^{46,h}, Y. Ding⁴⁰, Y. Ding³⁴, J. Dong^{1,58}, L. Y. Dong^{1,64}, M. Y. Dong^{1,58,64}, X. Dong⁷⁷, M. C. Du¹, S. X. Du⁸¹, Y. Y. Duan⁵⁵, Z. H. Duan⁴², P. Egorov^{36,b}, Y. H. Fan⁴⁵, J. Fang^{1,58}, J. Fang⁵⁹, S. S. Fang^{1,64}, W. X. Fang¹, Y. Fang¹, Y. Q. Fang^{1,58}, R. Farinelli^{29A}, L. Fava^{75B,75C}, F. Feldbauer³, G. Felici^{28A}, C. Q. Feng^{72,58}, J. H. Feng⁵⁹, Y. T. Feng^{72,58}, M. Fritsch³, C. D. Fu¹, J. L. Fu⁶⁴, Y. W. Fu^{1,64}, H. Gao⁶⁴, X. B. Gao⁴¹, Y. N. Gao^{46,h}, Yang Gao^{72,58}, S. Garbolino^{75C}, I. Garzia^{29A,29B}, L. Ge⁸¹, P. T. Ge¹⁹, Z. W. Ge⁴², C. Geng⁵⁹, E. M. Gersabeck⁶⁸, A. Gilman⁷⁰, K. Goetzen¹³, L. Gong⁴⁰, W. X. Gong^{1,58}, W. Gradl³⁵, S. Gramigna^{29A,29B}, M. Greco^{75A,75C}, M. H. Gu^{1,58}, Y. T. Gu¹⁵, C. Y. Guan^{1,64}, A. Q. Guo^{31,64}, L. B. Guo⁴¹, M. J. Guo⁵⁰, R. P. Guo⁴⁹, Y. P. Guo^{12,g}, A. Guskov^{36,b}, J. Gutierrez²⁷, K. L. Han⁶⁴, T. T. Han¹, F. Hanisch³, X. Q. Hao¹⁹, F. A. Harris⁶⁶, K. K. He⁵⁵, K. L. He^{1,64}, F. H. Heinsius³, C. H. Heinz³⁵, Y. K. Heng^{1,58,64}, C. Herold⁶⁰, T. Holtmann³, P. C. Hong³⁴, G. Y. Hou^{1,64}, X. T. Hou^{1,64}, Y. R. Hou⁶⁴, Z. L. Hou¹, B. Y. Hu⁵⁹, H. M. Hu^{1,64}, J. F. Hu^{56,j}, S. L. Hu^{12,g}, T. Hu^{1,58,64}, Y. Hu¹, G. S. Huang^{72,58}, K. X. Huang⁵⁹, L. Q. Huang^{31,64}, X. T. Huang⁵⁰, Y. P. Huang¹, Y. S. Huang⁵⁹, T. Hussain⁷⁴, F. Hölzken³, N. Hüskens³⁵, N. in der Wiesche⁶⁹, J. Jackson²⁷, S. Janchiv³², J. H. Jeong¹⁰, Q. Ji¹, Q. P. Ji¹⁹, W. Ji^{1,64}, X. B. Ji^{1,64}, X. L. Ji^{1,58}, Y. Y. Ji⁵⁰, X. Q. Jia⁵⁰, Z. K. Jia^{72,58}, D. Jiang^{1,64}, H. B. Jiang⁷⁷, P. C. Jiang^{46,h}, S. S. Jiang³⁹, T. J. Jiang¹⁶, X. S. Jiang^{1,58,64}, Y. Jiang⁶⁴, J. B. Jiao⁵⁰, J. K. Jiao³⁴, Z. Jiao²³, S. Jin⁴², Y. Jin⁶⁷, M. Q. Jing^{1,64}, X. M. Jing⁶⁴, T. Johansson⁷⁶, S. Kabana³³, N. Kalantar-Nayestanaki⁶⁵, X. L. Kang⁹, X. S. Kang⁴⁰, M. Kavatsyuk⁶⁵, B. C. Ke⁸¹, V. Khachatryan²⁷, A. Khoukaz⁶⁹, R. Kiuchi¹, O. B. Kolcu^{62A}, B. Kopf³, M. Kuessner³, X. Kui^{1,64}, N. Kumar²⁶, A. Kupsc^{44,76}, W. Kühn³⁷, J. J. Lane⁶⁸, L. Lavezzi^{75A,75C}, T. T. Lei^{72,58}, Z. H. Lei^{72,58}, M. Lellmann³⁵, T. Lenz³⁵, C. Li⁴⁷, C. Li⁴³, C. H. Li³⁹, Cheng Li^{72,58}, D. M. Li⁸¹, F. Li^{1,58}, G. Li¹, H. B. Li^{1,64}, H. J. Li¹⁹, H. N. Li^{56,j}, Hui Li⁴³, J. R. Li⁶¹, J. S. Li⁵⁹, K. Li¹, K. L. Li¹⁹, L. J. Li^{1,64}, L. K. Li¹, Lei Li⁴⁸, M. H. Li⁴³, P. R. Li^{38,k,l}, Q. M. Li^{1,64}, Q. X. Li⁵⁰, R. Li^{17,31}, S. X. Li¹², T. Li⁵⁰, W. D. Li^{1,64}, W. G. Li^{1,a}, X. Li^{1,64}, X. H. Li^{72,58}, X. L. Li⁵⁰, X. Y. Li^{1,64}, X. Z. Li⁵⁹, Y. G. Li^{46,h}, Z. J. Li⁵⁹, Z. Y. Li⁷⁹, C. Liang⁴², H. Liang^{72,58}, H. Liang^{1,64}, Y. F. Liang⁵⁴, Y. T. Liang^{31,64}, G. R. Liao¹⁴, Y. P. Liao^{1,64}, J. Libby²⁶, A. Limphirat⁶⁰, C. C. Lin⁵⁵, D. X. Lin^{31,64}, T. Lin¹, B. J. Liu¹, B. X. Liu⁷⁷, C. Liu³⁴, C. X. Liu¹, F. Liu¹, F. H. Liu⁵³, Feng Liu⁶, G. M. Liu^{56,j}, H. Liu^{38,k,l}, H. B. Liu¹⁵, H. H. Liu¹, H. M. Liu^{1,64}, Huihui Liu²¹, J. B. Liu^{72,58}, J. Y. Liu^{1,64}, K. Liu^{38,k,l}, K. Y. Liu⁴⁰, Ke Liu²², L. Liu^{72,58}, L. C. Liu⁴³, Lu Liu⁴³, M. H. Liu^{12,g}, P. L. Liu¹, Q. Liu⁶⁴, S. B. Liu^{72,58}, T. Liu^{12,g}, W. K. Liu⁴³, W. M. Liu^{72,58}, X. Liu^{38,k,l}, X. Liu³⁹, Y. Liu⁸¹, Y. Liu^{38,k,l}, Y. B. Liu⁴³, Z. A. Liu^{1,58,64}, Z. D. Liu⁹, Z. Q. Liu⁵⁰, X. C. Lou^{1,58,64}, F. X. Lu⁵⁹, H. J. Lu²³, J. G. Lu^{1,58}, X. L. Lu¹, Y. Lu⁷, Y. P. Lu^{1,58}, Z. H. Lu^{1,64}, C. L. Luo⁴¹, J. R. Luo⁵⁹, M. X. Luo⁸⁰, T. Luo^{12,g}, X. L. Luo^{1,58}, X. R. Lyu⁶⁴, Y. F. Lyu⁴³, F. C. Ma⁴⁰, H. Ma⁷⁹, H. L. Ma¹, J. L. Ma^{1,64}, L. L. Ma⁵⁰, L. R. Ma⁶⁷, M. M. Ma^{1,64}, Q. M. Ma¹, R. Q. Ma^{1,64}, T. Ma^{72,58}, X. T. Ma^{1,64}, X. Y. Ma^{1,58}, Y. M. Ma³¹, F. E. Maas¹⁸, I. MacKay⁷⁰, M. Maggiora^{75A,75C}, S. Malde⁷⁰, Y. J. Mao^{46,h}, Z. P. Mao¹, S. Marcello^{75A,75C}, Z. X. Meng⁶⁷, J. G. Messchendorp^{13,65}, G. Mezzadri^{29A}, H. Miao^{1,64}, T. J. Min⁴², R. E. Mitchell²⁷, X. H. Mo^{1,58,64}, B. Moses²⁷, N. Yu. Muchnoi^{4,c}, J. Muskalla³⁵, Y. Nefedov³⁶, F. Nerling^{18,e}, L. S. Nie²⁰, I. B. Nikolaev^{4,c}, Z. Ning^{1,58}, S. Nisar^{11,m}, Q. L. Niu^{38,k,l}, W. D. Niu⁵⁵, Y. Niu⁵⁰, S. L. Olsen⁶⁴, Q. Ouyang^{1,58,64}, S. Pacetti^{28B,28C}, X. Pan⁵⁵, Y. Pan⁵⁷, A. Pathak³⁴, Y. P. Pei^{72,58}, M. Pelizaeus³, H. P. Peng^{72,58}, Y. Y. Peng^{38,k,l}, K. Peters^{13,e}, J. L. Ping⁴¹, R. G. Ping^{1,64}, S. Plura³⁵, V. Prasad³³, F. Z. Qi¹, H. Qi^{72,58}, H. R. Qi⁶¹, M. Qi⁴², T. Y. Qi^{12,g}, S. Qian^{1,58}, W. B. Qian⁶⁴, C. F. Qiao⁶⁴, X. K. Qiao⁸¹, J. J. Qin⁷³, L. Q. Qin¹⁴, L. Y. Qin^{72,58}, X. P. Qin^{12,g}, X. S. Qin⁵⁰, Z. H. Qin^{1,58}, J. F. Qiu¹, Z. H. Qu⁷³, C. F. Redmer³⁵, K. J. Ren³⁹, A. Rivetti^{75C}, M. Rolo^{75C}, G. Rong^{1,64}, Ch. Rosner¹⁸, S. N. Ruan⁴³, N. Salone⁴⁴, A. Sarantsev^{36,d}, Y. Schelhaas³⁵, K. Schoenning⁷⁶, M. Scodreggio^{29A}, K. Y. Shan^{12,g}, W. Shan²⁴, X. Y. Shan^{72,58}, Z. J. Shang^{38,k,l}, J. F. Shangguan¹⁶, L. G. Shao^{1,64}, M. Shao^{72,58}, C. P. Shen^{12,g}, H. F. Shen^{1,8}, W. H. Shen⁶⁴, X. Y. Shen^{1,64}, B. A. Shi⁶⁴, H. Shi^{72,58}, H. C. Shi^{72,58}, J. L. Shi^{12,g}, J. Y. Shi¹, Q. Q. Shi⁵⁵, S. Y. Shi⁷³, X. Shi^{1,58}, J. J. Song¹⁹, T. Z. Song⁵⁹,

W. M. Song^{34,1}, Y. J. Song^{12,g}, Y. X. Song^{46,h,n}, S. Sosio^{75A,75C}, S. Spataro^{75A,75C}, F. Stieler³⁵, S. S. Su⁴⁰,
 Y. J. Su⁶⁴, G. B. Sun⁷⁷, G. X. Sun¹, H. Sun⁶⁴, H. K. Sun¹, J. F. Sun¹⁹, K. Sun⁶¹, L. Sun⁷⁷, S. S. Sun^{1,64},
 T. Sun^{51,f}, W. Y. Sun³⁴, Y. Sun⁹, Y. J. Sun^{72,58}, Y. Z. Sun¹, Z. Q. Sun^{1,64}, Z. T. Sun⁵⁰, C. J. Tang⁵⁴, G. Y. Tang¹,
 J. Tang⁵⁹, M. Tang^{72,58}, Y. A. Tang⁷⁷, L. Y. Tao⁷³, Q. T. Tao^{25,i}, M. Tat⁷⁰, J. X. Teng^{72,58}, V. Thoren⁷⁶,
 W. H. Tian⁵⁹, Y. Tian^{31,64}, Z. F. Tian⁷⁷, I. Uman^{62B}, Y. Wan⁵⁵, S. J. Wang⁵⁰, B. Wang¹, B. L. Wang⁶⁴,
 Bo Wang^{72,58}, D. Y. Wang^{46,h}, F. Wang⁷³, H. J. Wang^{38,k,l}, J. J. Wang⁷⁷, J. P. Wang⁵⁰, K. Wang^{1,58}, L. L. Wang¹,
 M. Wang⁵⁰, N. Y. Wang⁶⁴, S. Wang^{12,g}, S. Wang^{38,k,l}, T. Wang^{12,g}, T. J. Wang⁴³, W. Wang⁷³, W. Wang⁵⁹,
 W. P. Wang^{35,58,72,o}, X. Wang^{46,h}, X. F. Wang^{38,k,l}, X. J. Wang³⁹, X. L. Wang^{12,g}, X. N. Wang¹, Y. Wang⁶¹,
 Y. D. Wang⁴⁵, Y. F. Wang^{1,58,64}, Y. L. Wang¹⁹, Y. N. Wang⁴⁵, Y. Q. Wang¹, Yaqian Wang¹⁷, Yi Wang⁶¹,
 Z. Wang^{1,58}, Z. L. Wang⁷³, Z. Y. Wang^{1,64}, Ziyi Wang⁶⁴, D. H. Wei¹⁴, F. Weidner⁶⁹, S. P. Wen¹, Y. R. Wen³⁹,
 U. Wiedner³, G. Wilkinson⁷⁰, M. Wolke⁷⁶, L. Wollenberg³, C. Wu³⁹, J. F. Wu^{1,8}, L. H. Wu¹, L. J. Wu^{1,64},
 X. Wu^{12,g}, X. H. Wu³⁴, Y. Wu^{72,58}, Y. H. Wu⁵⁵, Y. J. Wu³¹, Z. Wu^{1,58}, L. Xia^{72,58}, X. M. Xian³⁹, B. H. Xiang^{1,64},
 T. Xiang^{46,h}, D. Xiao^{38,k,l}, G. Y. Xiao⁴², S. Y. Xiao¹, Y. L. Xiao^{12,g}, Z. J. Xiao⁴¹, C. Xie⁴², X. H. Xie^{46,h},
 Y. Xie⁵⁰, Y. G. Xie^{1,58}, Y. H. Xie⁶, Z. P. Xie^{72,58}, T. Y. Xing^{1,64}, C. F. Xu^{1,64}, C. J. Xu⁵⁹, G. F. Xu¹,
 H. Y. Xu^{67,2,p}, M. Xu^{72,58}, Q. J. Xu¹⁶, Q. N. Xu³⁰, W. Xu¹, W. L. Xu⁶⁷, X. P. Xu⁵⁵, Y. Xu⁴⁰, Y. C. Xu⁷⁸,
 Z. S. Xu⁶⁴, F. Yan^{12,g}, L. Yan^{12,g}, W. B. Yan^{72,58}, W. C. Yan⁸¹, X. Q. Yan^{1,64}, H. J. Yang^{51,f}, H. L. Yang³⁴,
 H. X. Yang¹, T. Yang¹, Y. Yang^{12,g}, Y. F. Yang⁴³, Y. F. Yang^{1,64}, Y. X. Yang^{1,64}, Z. W. Yang^{38,k,l}, Z. P. Yao⁵⁰,
 M. Ye^{1,58}, M. H. Ye⁸, J. H. Yin¹, Junhao Yin⁴³, Z. Y. You⁵⁹, B. X. Yu^{1,58,64}, C. X. Yu⁴³, G. Yu^{1,64}, J. S. Yu^{25,i},
 M. C. Yu⁴⁰, T. Yu⁷³, X. D. Yu^{46,h}, Y. C. Yu⁸¹, C. Z. Yuan^{1,64}, J. Yuan³⁴, J. Yuan⁴⁵, L. Yuan², S. C. Yuan^{1,64},
 Y. Yuan^{1,64}, Z. Y. Yuan⁵⁹, C. X. Yue³⁹, A. A. Zafar⁷⁴, F. R. Zeng⁵⁰, S. H. Zeng^{63A,63B,63C,63D}, X. Zeng^{12,g},
 Y. Zeng^{25,i}, Y. J. Zeng^{1,64}, Y. J. Zeng⁵⁹, X. Y. Zhai³⁴, Y. C. Zhai⁵⁰, Y. H. Zhan⁵⁹, A. Q. Zhang^{1,64},
 B. L. Zhang^{1,64}, B. X. Zhang¹, D. H. Zhang⁴³, G. Y. Zhang¹⁹, H. Zhang⁸¹, H. Zhang^{72,58}, H. C. Zhang^{1,58,64},
 H. H. Zhang⁵⁹, H. H. Zhang³⁴, H. Q. Zhang^{1,58,64}, H. R. Zhang^{72,58}, H. Y. Zhang^{1,58}, J. Zhang⁵⁹, J. Zhang⁸¹,
 J. J. Zhang⁵², J. L. Zhang²⁰, J. Q. Zhang⁴¹, J. S. Zhang^{12,g}, J. W. Zhang^{1,58,64}, J. X. Zhang^{38,k,l}, J. Y. Zhang¹,
 J. Z. Zhang^{1,64}, Jianyu Zhang⁶⁴, L. M. Zhang⁶¹, Lei Zhang⁴², P. Zhang^{1,64}, Q. Y. Zhang³⁴, R. Y. Zhang^{38,k,l},
 S. H. Zhang^{1,64}, Shulei Zhang^{25,i}, X. D. Zhang⁴⁵, X. M. Zhang¹, X. Y. Zhang⁴⁰, X. Y. Zhang⁵⁰, Y. Zhang¹, Y.
 Zhang⁷³, Y. T. Zhang⁸¹, Y. H. Zhang^{1,58}, Y. M. Zhang³⁹, Yan Zhang^{72,58}, Z. D. Zhang¹, Z. H. Zhang¹,
 Z. L. Zhang³⁴, Z. Y. Zhang⁷⁷, Z. Y. Zhang⁴³, Z. Z. Zhang⁴⁵, G. Zhao¹, J. Y. Zhao^{1,64}, J. Z. Zhao^{1,58}, L. Zhao¹,
 Lei Zhao^{72,58}, M. G. Zhao⁴³, N. Zhao⁷⁹, R. P. Zhao⁶⁴, S. J. Zhao⁸¹, Y. B. Zhao^{1,58}, Y. X. Zhao^{31,64}, Z. G. Zhao^{72,58},
 A. Zhemchugov^{36,b}, B. Zheng⁷³, B. M. Zheng³⁴, J. P. Zheng^{1,58}, W. J. Zheng^{1,64}, Y. H. Zheng⁶⁴, B. Zhong⁴¹,
 X. Zhong⁵⁹, H. Zhou⁵⁰, J. Y. Zhou³⁴, L. P. Zhou^{1,64}, S. Zhou⁶, X. Zhou⁷⁷, X. K. Zhou⁶, X. R. Zhou^{72,58},
 X. Y. Zhou³⁹, Y. Z. Zhou^{12,g}, Z. C. Zhou²⁰, A. N. Zhu⁶⁴, J. Zhu⁴³, K. Zhu¹, K. J. Zhu^{1,58,64}, K. S. Zhu^{12,g},
 L. Zhu³⁴, L. X. Zhu⁶⁴, S. H. Zhu⁷¹, T. J. Zhu^{12,g}, W. D. Zhu⁴¹, Y. C. Zhu^{72,58}, Z. A. Zhu^{1,64}, J. H. Zou¹, J. Zu^{72,58}

(BESIII Collaboration)

¹ *Institute of High Energy Physics, Beijing 100049, People's Republic of China*

² *Beihang University, Beijing 100191, People's Republic of China*

³ *Bochum Ruhr-University, D-44780 Bochum, Germany*

⁴ *Budker Institute of Nuclear Physics SB RAS (BINP), Novosibirsk 630090, Russia*

⁵ *Carnegie Mellon University, Pittsburgh, Pennsylvania 15213, USA*

⁶ *Central China Normal University, Wuhan 430079, People's Republic of China*

⁷ *Central South University, Changsha 410083, People's Republic of China*

⁸ *China Center of Advanced Science and Technology, Beijing 100190, People's Republic of China*

⁹ *China University of Geosciences, Wuhan 430074, People's Republic of China*

¹⁰ *Chung-Ang University, Seoul, 06974, Republic of Korea*

¹¹ *COMSATS University Islamabad, Lahore Campus, Defence Road, Off Raiwind Road, 54000 Lahore, Pakistan*

¹² *Fudan University, Shanghai 200433, People's Republic of China*

¹³ *GSI Helmholtzcentre for Heavy Ion Research GmbH, D-64291 Darmstadt, Germany*

¹⁴ *Guangxi Normal University, Guilin 541004, People's Republic of China*

¹⁵ *Guangxi University, Nanning 530004, People's Republic of China*

¹⁶ *Hangzhou Normal University, Hangzhou 310036, People's Republic of China*

¹⁷ *Hebei University, Baoding 071002, People's Republic of China*

¹⁸ *Helmholtz Institute Mainz, Staudinger Weg 18, D-55099 Mainz, Germany*

¹⁹ *Henan Normal University, Xinxiang 453007, People's Republic of China*

- ²⁰ Henan University, Kaifeng 475004, People's Republic of China
- ²¹ Henan University of Science and Technology, Luoyang 471003, People's Republic of China
- ²² Henan University of Technology, Zhengzhou 450001, People's Republic of China
- ²³ Huangshan College, Huangshan 245000, People's Republic of China
- ²⁴ Hunan Normal University, Changsha 410081, People's Republic of China
- ²⁵ Hunan University, Changsha 410082, People's Republic of China
- ²⁶ Indian Institute of Technology Madras, Chennai 600036, India
- ²⁷ Indiana University, Bloomington, Indiana 47405, USA
- ²⁸ INFN Laboratori Nazionali di Frascati, (A)INFN Laboratori Nazionali di Frascati, I-00044, Frascati, Italy; (B)INFN Sezione di Perugia, I-06100, Perugia, Italy; (C)University of Perugia, I-06100, Perugia, Italy
- ²⁹ INFN Sezione di Ferrara, (A)INFN Sezione di Ferrara, I-44122, Ferrara, Italy; (B)University of Ferrara, I-44122, Ferrara, Italy
- ³⁰ Inner Mongolia University, Hohhot 010021, People's Republic of China
- ³¹ Institute of Modern Physics, Lanzhou 730000, People's Republic of China
- ³² Institute of Physics and Technology, Peace Avenue 54B, Ulaanbaatar 13330, Mongolia
- ³³ Instituto de Alta Investigación, Universidad de Tarapacá, Casilla 7D, Arica 1000000, Chile
- ³⁴ Jilin University, Changchun 130012, People's Republic of China
- ³⁵ Johannes Gutenberg University of Mainz, Johann-Joachim-Becher-Weg 45, D-55099 Mainz, Germany
- ³⁶ Joint Institute for Nuclear Research, 141980 Dubna, Moscow region, Russia
- ³⁷ Justus-Liebig-Universität Giessen, II. Physikalisches Institut, Heinrich-Buff-Ring 16, D-35392 Giessen, Germany
- ³⁸ Lanzhou University, Lanzhou 730000, People's Republic of China
- ³⁹ Liaoning Normal University, Dalian 116029, People's Republic of China
- ⁴⁰ Liaoning University, Shenyang 110036, People's Republic of China
- ⁴¹ Nanjing Normal University, Nanjing 210023, People's Republic of China
- ⁴² Nanjing University, Nanjing 210093, People's Republic of China
- ⁴³ Nankai University, Tianjin 300071, People's Republic of China
- ⁴⁴ National Centre for Nuclear Research, Warsaw 02-093, Poland
- ⁴⁵ North China Electric Power University, Beijing 102206, People's Republic of China
- ⁴⁶ Peking University, Beijing 100871, People's Republic of China
- ⁴⁷ Qufu Normal University, Qufu 273165, People's Republic of China
- ⁴⁸ Renmin University of China, Beijing 100872, People's Republic of China
- ⁴⁹ Shandong Normal University, Jinan 250014, People's Republic of China
- ⁵⁰ Shandong University, Jinan 250100, People's Republic of China
- ⁵¹ Shanghai Jiao Tong University, Shanghai 200240, People's Republic of China
- ⁵² Shanxi Normal University, Linfen 041004, People's Republic of China
- ⁵³ Shanxi University, Taiyuan 030006, People's Republic of China
- ⁵⁴ Sichuan University, Chengdu 610064, People's Republic of China
- ⁵⁵ Soochow University, Suzhou 215006, People's Republic of China
- ⁵⁶ South China Normal University, Guangzhou 510006, People's Republic of China
- ⁵⁷ Southeast University, Nanjing 211100, People's Republic of China
- ⁵⁸ State Key Laboratory of Particle Detection and Electronics, Beijing 100049, Hefei 230026, People's Republic of China
- ⁵⁹ Sun Yat-Sen University, Guangzhou 510275, People's Republic of China
- ⁶⁰ Suranaree University of Technology, University Avenue 111, Nakhon Ratchasima 30000, Thailand
- ⁶¹ Tsinghua University, Beijing 100084, People's Republic of China
- ⁶² Turkish Accelerator Center Particle Factory Group, (A)Istinye University, 34010, Istanbul, Turkey; (B)Near East University, Nicosia, North Cyprus, 99138, Mersin 10, Turkey
- ⁶³ University of Bristol, (A)H H Wills Physics Laboratory; (B)Tyndall Avenue; (C)Bristol; (D)BS8 1TL
- ⁶⁴ University of Chinese Academy of Sciences, Beijing 100049, People's Republic of China
- ⁶⁵ University of Groningen, NL-9747 AA Groningen, The Netherlands
- ⁶⁶ University of Hawaii, Honolulu, Hawaii 96822, USA
- ⁶⁷ University of Jinan, Jinan 250022, People's Republic of China

⁶⁸ *University of Manchester, Oxford Road, Manchester, M13 9PL, United Kingdom*

⁶⁹ *University of Muenster, Wilhelm-Klemm-Strasse 9, 48149 Muenster, Germany*

⁷⁰ *University of Oxford, Keble Road, Oxford OX13RH, United Kingdom*

⁷¹ *University of Science and Technology Liaoning, Anshan 114051, People's Republic of China*

⁷² *University of Science and Technology of China, Hefei 230026, People's Republic of China*

⁷³ *University of South China, Hengyang 421001, People's Republic of China*

⁷⁴ *University of the Punjab, Lahore-54590, Pakistan*

⁷⁵ *University of Turin and INFN, (A)University of Turin, I-10125, Turin, Italy; (B)University of Eastern Piedmont, I-15121, Alessandria, Italy; (C)INFN, I-10125, Turin, Italy*

⁷⁶ *Uppsala University, Box 516, SE-75120 Uppsala, Sweden*

⁷⁷ *Wuhan University, Wuhan 430072, People's Republic of China*

⁷⁸ *Yantai University, Yantai 264005, People's Republic of China*

⁷⁹ *Yunnan University, Kunming 650500, People's Republic of China*

⁸⁰ *Zhejiang University, Hangzhou 310027, People's Republic of China*

⁸¹ *Zhengzhou University, Zhengzhou 450001, People's Republic of China*

^a *Deceased*

^b *Also at the Moscow Institute of Physics and Technology, Moscow 141700, Russia*

^c *Also at the Novosibirsk State University, Novosibirsk, 630090, Russia*

^d *Also at the NRC "Kurchatov Institute", PNPI, 188300, Gatchina, Russia*

^e *Also at Goethe University Frankfurt, 60323 Frankfurt am Main, Germany*

^f *Also at Key Laboratory for Particle Physics, Astrophysics and Cosmology, Ministry of Education; Shanghai Key Laboratory for Particle Physics and Cosmology; Institute of Nuclear and Particle Physics, Shanghai 200240, People's Republic of China*

^g *Also at Key Laboratory of Nuclear Physics and Ion-beam Application (MOE) and Institute of Modern Physics, Fudan University, Shanghai 200443, People's Republic of China*

^h *Also at State Key Laboratory of Nuclear Physics and Technology, Peking University, Beijing 100871, People's Republic of China*

ⁱ *Also at School of Physics and Electronics, Hunan University, Changsha 410082, China*

^j *Also at Guangdong Provincial Key Laboratory of Nuclear Science, Institute of Quantum Matter, South China Normal University, Guangzhou 510006, China*

^k *Also at MOE Frontiers Science Center for Rare Isotopes, Lanzhou University, Lanzhou 730000, People's Republic of China*

^l *Also at Lanzhou Center for Theoretical Physics, Lanzhou University, Lanzhou 730000, People's Republic of China*

^m *Also at the Department of Mathematical Sciences, IBA, Karachi 75270, Pakistan*

ⁿ *Also at Ecole Polytechnique Federale de Lausanne (EPFL), CH-1015 Lausanne, Switzerland*

^o *Also at Helmholtz Institute Mainz, Staudinger Weg 18, D-55099 Mainz, Germany*

^p *Also at School of Physics, Beihang University, Beijing 100191, China*

Based on $(2712.4 \pm 14.1) \times 10^6$ $\psi(2S)$ events, 7.9 fb^{-1} $\psi(3773)$ data, and 0.8 fb^{-1} off-resonance data samples collected with the BESIII detector, we measure the branching fraction of $\psi(2S) \rightarrow \gamma\pi^0$ and $e^+e^- \rightarrow \gamma\pi^0$ form factor at momentum transfers $Q^2 \sim 13 \text{ GeV}^2$. The $e^+e^- \rightarrow \gamma\pi^0$ cross section is fitted with considering the interference between the $\psi(2S)$ and continuum amplitudes and two solutions are found, $\mathcal{B} = 3.74 \times 10^{-7}$ with $\phi = 3.93 \text{ rad}$ and $\mathcal{B} = 7.87 \times 10^{-7}$ with $\phi = 2.08 \text{ rad}$. Here, \mathcal{B} is the branching fraction of $\psi(2S) \rightarrow \gamma\pi^0$ and ϕ is the relative phase angle between the $\psi(2S)$ and continuum amplitudes. Due to insufficient off-resonance data, the branching fraction $\mathcal{B}(\psi(2S) \rightarrow \gamma\pi^0)$ is determined to be in the range $[2.7, 9.7] \times 10^{-7}$ within one standard deviation of the contour region.

I. INTRODUCTION

Within the framework of Quantum Chromodynamics (QCD), vector charmonium radiative decays are believed to proceed mainly via short-distance $c\bar{c}$ annihilations into two gluons with a photon emitted by charm quarks [1]. However, when considering vector charmonium radiative

decay to a light pseudoscalar, other phenomenological mechanisms become important, such as the mixing of $\eta_c - \eta^{(\prime)}$ [2, 3], final state radiation by light quarks [4], and the vector meson dominance (VMD) model [4, 5]. Measurements of these charmonium radiative decays provide tests for various theoretical predictions.

The decay rate of $\psi(2S) \rightarrow \gamma\pi^0$ is expected to be

smaller than those of $\psi(2S) \rightarrow \gamma\eta$ and $\gamma\eta'$ due to the suppressed gluon coupling to isovector currents [4]. BESIII has measured the branching fractions of decays $\psi(2S) \rightarrow \gamma\pi^0$, $\gamma\eta$, and $\gamma\eta'$ and reported $\mathcal{B}(\psi(2S) \rightarrow \gamma\pi^0) = (9.5 \pm 1.6 \pm 0.5) \times 10^{-7}$ [6]. The branching fractions of $\psi(2S) \rightarrow \gamma\eta$ and $\gamma\eta'$ are well understood using the VMD model associated with the mixing of $\eta_c - \eta^{(\prime)}$. However, the branching fraction of $\psi(2S) \rightarrow \gamma\pi^0$ is one order of magnitude larger than the predicted range of $(0.66 \sim 1.15) \times 10^{-7}$ from the VMD model [7].

This discrepancy may arise from the irreducible background contribution from the continuum amplitude of $e^+e^- \rightarrow \gamma^* \rightarrow \gamma\pi^0$. In the recent BESIII measurement [6], the contribution from the continuum amplitude was not considered due to insufficient data samples at off-resonance energy points, and the continuum itself and its interference with the $\psi(2S)$ decay amplitude were neglected. With increased statistics of both off-resonance and resonance data, the interference effect can now be taken into account, and the $e^+e^- \rightarrow \gamma^* \rightarrow \gamma\pi^0$ form factor can be measured through the continuum process $e^+e^- \rightarrow \gamma^* \rightarrow \gamma\pi^0$. This allows for a more reliable determination of branching fraction of $\psi(2S) \rightarrow \gamma\pi^0$.

The cross section for the process $e^+e^- \rightarrow \gamma^* \rightarrow \gamma\pi^0$ at center-of-mass (c.m.) energy \sqrt{s} is given by

$$\sigma(s) = \frac{2\pi^2\alpha^3}{3} |F_{\pi^0}(s)|^2, \quad (1)$$

where F_{π^0} is the π^0 transition form factor and α is fine-structure constant. The form factor F_{π^0} is calculated using perturbative quantum chromodynamics (pQCD) in the asymptotic limit [8, 9],

$$-Q^2 F_{\pi^0}(Q^2) = \sqrt{2} f_{\pi^0} \left(1 - \frac{5}{3} \frac{\alpha_s(Q^2)}{\pi} \right), \quad Q^2 \gg m_{\pi^0}^2, \quad (2)$$

where $Q^2 = -q^2$, q is the four-momentum of the virtual photon, f_{π^0} is the π^0 decay constant, m_{π^0} is the mass of π^0 [10], and α_s is the strong coupling. This measurement provides a critical test of pQCD predictions [8, 9].

In this paper, we measure the branching fraction of $\psi(2S) \rightarrow \gamma\pi^0$ based on 2.7 billion $\psi(2S)$ events, 7.9 fb $^{-1}$ $\psi(3773)$ data, and 0.8 fb $^{-1}$ off-resonance data samples collected at $\sqrt{s} = 3.650$ and 3.682 GeV with the BESIII detector operating at the BEPCII [11–13].

II. BESIII DETECTOR AND MC SIMULATION

The BESIII detector [14] records symmetric e^+e^- collisions provided by the BEPCII storage ring [15] in the c.m. energy range from 1.84 to 4.95 GeV, with a peak luminosity of 1.1×10^{33} cm $^{-2}$ s $^{-1}$ achieved at $\sqrt{s} = 3.773$ GeV. BESIII has collected large data samples in this energy region [16–18]. The cylindrical core of the BESIII detector covers 93% of the full solid angle and consists of a helium-based multilayer drift chamber (MDC), a plastic scintillator time-of-flight system (TOF), and a CsI(Tl) electromagnetic calorimeter (EMC), which are all enclosed in

a superconducting solenoidal magnet providing a 1.0 T magnetic field. The solenoid is supported by an octagonal flux-return yoke with resistive plate counter muon identification modules interleaved with steel. The charged-particle momentum resolution at 1 GeV/c is 0.5%, and the dE/dx resolution is 6% for electrons from Bhabha scattering. The EMC measures photon energies with a resolution of 2.5% (5%) at 1 GeV in the barrel (end cap) region. The time resolution in the TOF barrel region is 68 ps, while that in the end cap region was 110 ps. The end cap TOF system was upgraded in 2015 using multi-gap resistive plate chamber technology, providing a time resolution of 60 ps, which benefits 84% of the data used in this analysis [19–21].

Monte Carlo (MC) simulated data samples produced with a GEANT4-based [22] software package, which includes the geometric description of the BESIII detector and the detector response, are used to determine detection efficiencies and to estimate backgrounds. The simulation models the beam energy spread and initial state radiation (ISR) in the e^+e^- annihilations with the generator KKMC [23, 24]. Inclusive MC simulations are used to estimate backgrounds including the production of the $\psi(2S)$ resonance, the production of $D\bar{D}$ pairs (including quantum coherence for the neutral D channels), the non- $D\bar{D}$ decays of the $\psi(3770)$, the ISR production, and the continuum processes incorporated in KKMC [23, 24]. All particle decays are modeled with EVTGEN [25, 26] using branching fractions either taken from the Particle Data Group [10], when available, or otherwise estimated with LUNDCHARM [27, 28]. Final state radiation (FSR) from charged final state particles is incorporated using the PHOTOS package [29]. The signal MC for $e^+e^- \rightarrow \gamma\pi^0$ is generated to determine the efficiency using the helicity amplitude (HELAMP) model with the EVTGEN [25, 26].

III. EVENT SELECTION

The π^0 is reconstructed with two photons so there are three photons in the final state and no good charged tracks.

Good charged tracks detected in the MDC are required to be within a polar angle (θ) range of $|\cos\theta| < 0.93$, where θ is defined with respect to the z -axis, which is the symmetry axis of the MDC. The distance of closest approach to the interaction point (IP) must be less than 10 cm along the z -axis, and less than 1 cm in the transverse plane.

Photon candidates are identified using isolated showers in the EMC. The photons are required to be only in barrel EMC ($|\cos\theta| < 0.8$) to suppress the backgrounds from the quantum electrodynamics (QED) processes and the deposited energy of each photon in EMC should be more than 25 MeV. The number of photons is required to be exactly 3, which can suppress most backgrounds that involve more than 3 photons in the final state. A four-constraint (4C) kinematic fit with the constraints

provided by four-momentum conservation is imposed on the three photons, and χ_{4C}^2 is required to be less than 40. The photon with the highest energy is regarded as the radiative photon and other two photons with lower energy are regarded as the π^0 candidates. To further suppress backgrounds from the QED process $e^+e^- \rightarrow \gamma\gamma\gamma$, the cosine of the helicity angle of γ is required to be less than 0.7. The helicity angle is defined as the angle between the momentum of the γ from π^0 with larger deposited energy in the π^0 rest frame and the momentum of π^0 in the e^+e^- c.m. frame.

The background is studied with inclusive $\psi(2S)$ MC samples and QED processes $e^+e^- \rightarrow \gamma\gamma(\gamma_{\text{ISR}})$ generated at each energy point. The dominant backgrounds are the $e^+e^- \rightarrow \gamma\gamma$ events where one photon converts into an e^+e^- pair, and if the track finding algorithm fails, electrons and positrons can be misidentified as two photons. An example of a γ -conversion event in the $x-y$ plane is displayed in Fig. 1. Figure 2 shows the two-dimensional distribution of the number of hits versus the $\gamma\gamma$ invariant mass ($m_{\gamma\gamma}$) in the $\psi(2S)$ data and MC simulation. To suppress these background events, the number of hits in the MDC in the region between the two radial lines connecting the IP and the two shower positions in the EMC is required to be less than 8 [30]. Most of the γ -conversion events from the $e^+e^- \rightarrow \gamma\gamma$ process can be rejected. After applying the above requirements, the remaining peaking backgrounds come from $\psi(2S) \rightarrow \gamma\chi_{cJ}$ decays with $\chi_{cJ} \rightarrow \pi^0\pi^0$, where $J=0$ or 2. The contribution from these peaking backgrounds is estimated precisely using the well-measured branching fractions [10]. The selection efficiencies are 0.017% and 0.045% for $\psi(2S) \rightarrow \gamma\chi_{c0}$ and $\psi(2S) \rightarrow \gamma\chi_{c2}$, respectively. The expected numbers are 125.1 ± 12.5 for $\psi(2S) \rightarrow \gamma\chi_{c0}$ and 85.6 ± 10.0 for $\psi(2S) \rightarrow \gamma\chi_{c2}$. The other remaining smooth backgrounds are from QED processes ($e^+e^- \rightarrow \gamma\gamma\gamma(n\gamma)$, $n \geq 0$). Due to the inefficiency of the reconstruction algorithms of photons, background events with more than three photon candidates still survive after requiring exactly three photon candidates.

To extract the number of signal events, an unbinned maximum likelihood fit is performed on the $m_{\gamma\gamma}$ spectrum for each dataset. When calculating $m_{\gamma\gamma}$, the measured momentum of γ is used instead of the momentum modified by 4C kinematic fit to avoid possible bias.

For the fit to $m_{\gamma\gamma}$ at $\sqrt{s} = 3.686$ GeV, the probability density function (P.D.F.) consists of three components: the signal, the peaking background from $\psi(2S) \rightarrow \gamma\chi_{cJ}$ decays with $\chi_{cJ} \rightarrow \pi^0\pi^0$, and the smooth background from QED processes ($e^+e^- \rightarrow \gamma\gamma\gamma(n\gamma)$, $n \geq 0$). The signal is modeled using a MC-simulated shape convolved with a Gaussian function to account for the difference in mass resolution between data and MC simulation. The mean and standard deviation of the Gaussian function are free in the fit. The peaking background is described by the MC-simulated shape, and the number of peaking background events is fixed to the expected value from MC studies. The smooth background is described by

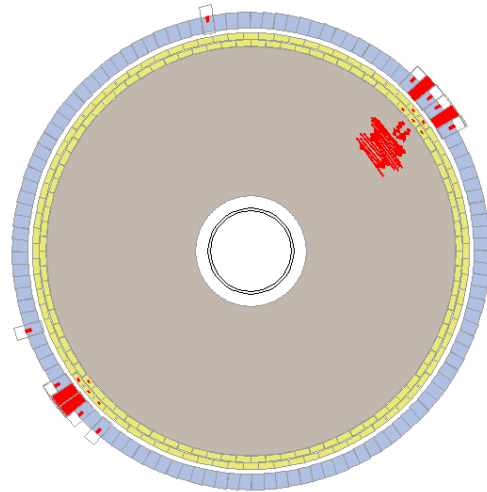


FIG. 1. The view of a γ -conversion event in the MDC and EMC in $x-y$ plane.

a third-order Chebychev polynomial function with shape parameters obtained from MC-simulated QED processes.

For the fits at $\sqrt{s} = 3.650, 3.682,$ and 3.773 GeV, the P.D.F only consists of a signal and a smooth background from MC-simulated QED processes. The parameters of the Gaussian function in the signal shape at $\sqrt{s} = 3.650$ and 3.682 GeV are constrained to the values obtained from the fit at $\sqrt{s} = 3.686$ GeV due to limited statistics at these energies.

The fit results at each c.m. energy are shown in Fig. 3. The statistical significances are $12.2\sigma, 2.4\sigma, 1.8\sigma,$ and 6.2σ in comparison to an alternative fit without including the signal shape at $\sqrt{s} = 3.686, 3.650, 3.682,$ and 3.773 GeV, respectively. The signal yields and the observed cross sections for all data samples are summarized in Table I.

IV. BRANCHING FRACTION MEASUREMENT

At each c.m. energy, the observed cross section is calculated with

$$\sigma^{\text{obs}} = \frac{N^{\text{sig}}}{L \cdot \epsilon \cdot \mathcal{B}_{\pi^0 \rightarrow \gamma\gamma}}, \quad (3)$$

where N^{sig} is the number of signal events obtained from the fit to the $m_{\gamma\gamma}$ distribution as described in Sec. III, L is the integrated luminosity, ϵ is the selection efficiency, and $\mathcal{B}_{\pi^0 \rightarrow \gamma\gamma}$ is the branching fraction of $\pi^0 \rightarrow \gamma\gamma$ taken from PDG [10]. The efficiency is estimated by an iterative weighting method [31] and results are shown in Table I.

The cross section of $e^+e^- \rightarrow \gamma\pi^0$ near the vicinity of the $\psi(2S)$ peak is a coherent sum of the continuum

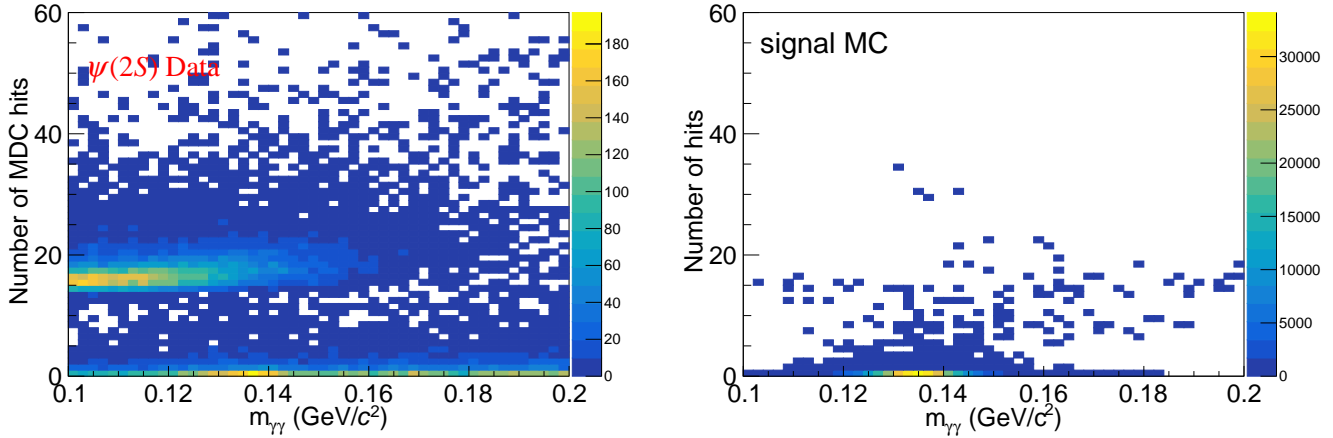


FIG. 2. Two-dimensional distributions of the number of hits versus $m_{\gamma\gamma}$ in $\psi(2S)$ data (left panel) and MC-simulated signal process (right panel).

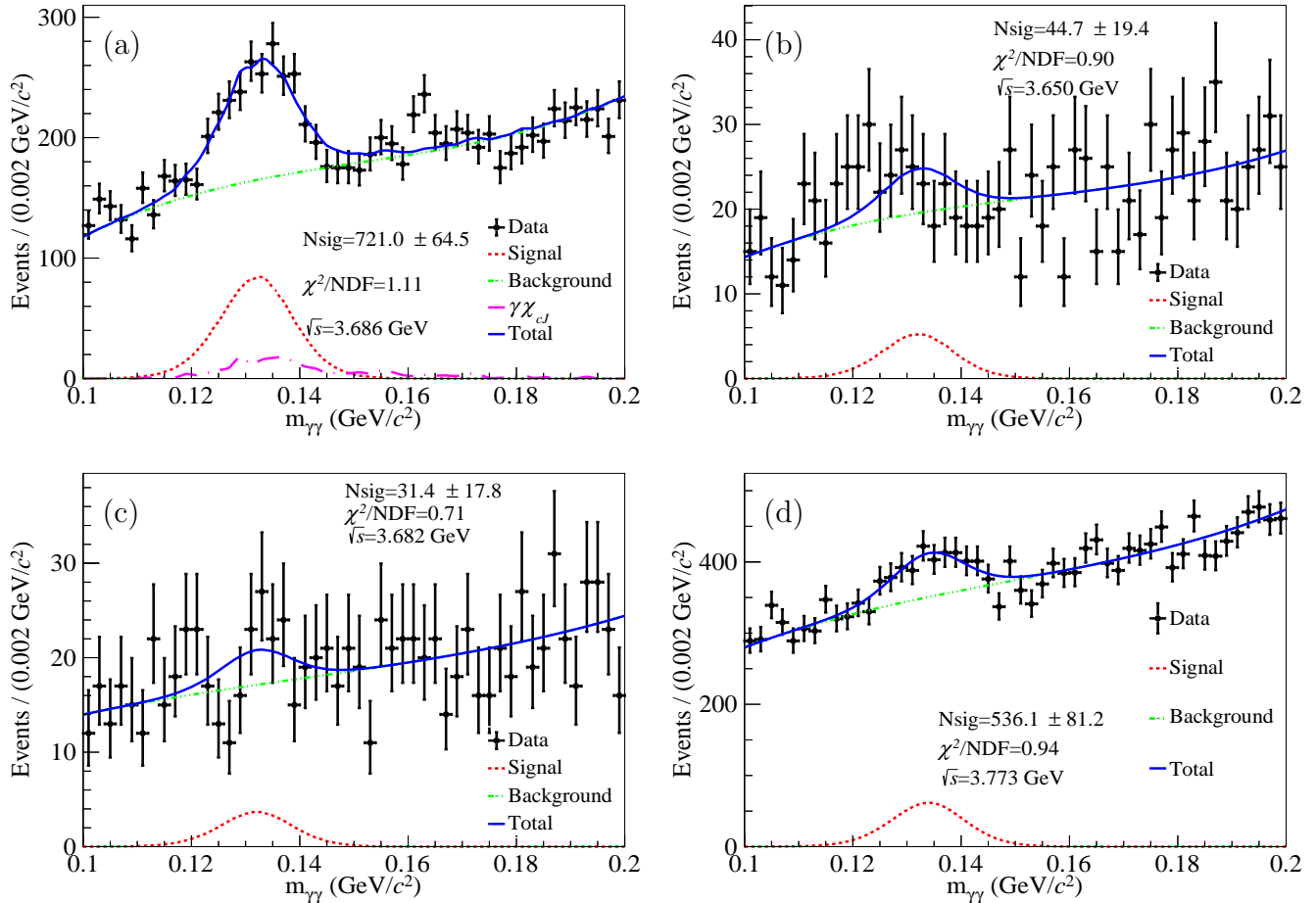


FIG. 3. The fit to the $m_{\gamma\gamma}$ at the c.m. energy points of (a) $\psi(2S)$; (b) $\sqrt{s} = 3.650$ GeV; (c) $\sqrt{s} = 3.682$ GeV; (d) $\sqrt{s} = 3.773$ GeV. Dots with error bars represent data, blue solid curves represent fit results, red dashed curves represent signal MC simulation, green dashed curves represent QED background contributions, and the pink dash-dotted curve represents peaking background from $\psi(2S) \rightarrow \gamma\chi_{cJ}$ decays.

TABLE I. The signal yields and the observed cross sections at each c.m. energy, where N^{sig} is the signal yield, L is the integrated luminosity, ϵ is selection efficiency, and σ^{obs} is the observed cross section.

\sqrt{s} (GeV)	L (pb $^{-1}$)	N^{sig}	ϵ (%)	σ^{obs} (pb)
3.650	401	44.7 ± 19.4	29.00	0.38 ± 0.17
3.682	392	31.4 ± 17.8	29.86	0.27 ± 0.15
3.686	3877	721.0 ± 64.5	30.62	0.61 ± 0.05
3.773	7909	536.1 ± 81.2	30.84	0.22 ± 0.03

amplitude and the resonance amplitude of $\psi(2S)$ which is given by

$$\sigma_{\text{tot}}(s) = \frac{4\pi\alpha^2 s}{3} \left| \frac{f \cdot e^{i\phi}}{s^{\frac{3}{2}}} \sqrt{\frac{\alpha\pi}{2}} + \frac{3}{\sqrt{s}\alpha} \frac{\sqrt{\Gamma_{\psi(2S)}\Gamma_{ee}\mathcal{B}(\psi(2S) \rightarrow \gamma\pi^0)}}{s - M^2 + iM\Gamma_{\psi(2S)}} \right|^2, \quad (4)$$

where the first term is the contribution of $e^+e^- \rightarrow \gamma^* \rightarrow \gamma\pi^0$ with the $F_{\pi^0}(s)$ in Eq.(1) parameterized as $\frac{f}{s}$, where f is a free parameter in the fit. The second term is the relativistic Breit-Wigner function of $\psi(2S)$, ϕ is the relative phase between the $\psi(2S)$ and continuum amplitudes, $\Gamma_{\psi(2S)}$, Γ_{ee} , and M are the total width, e^+e^- partial width, and mass of $\psi(2S)$, respectively, and are fixed to their PDG values [10]. As $\psi(2S)$ is a narrow resonance, ISR and beam energy spread are taken into account in the fit and the final expression of the cross section is given by [32]

$$\sigma_{\text{exp}} = \int_0^{x_m} dx \int_{\sqrt{s}-50\Delta}^{\sqrt{s}+50\Delta} d\sqrt{s'} F(x, s') \sigma_{\text{tot}}(s'(1-x)) G(\sqrt{s}, \sqrt{s'}),$$

$$G(\sqrt{s}, \sqrt{s'}) = \frac{1}{\sqrt{2\pi}\Delta} e^{-\frac{(\sqrt{s}-\sqrt{s'})^2}{2\Delta^2}}, \quad (5)$$

$$F(x, s) = x^{\beta-1} \beta \cdot (1 + \delta) - \beta(1 - \frac{x}{2}) + \frac{1}{8}\beta^2 \left[4 \cdot (2-x) \cdot \ln \frac{1}{x} - \frac{1+3(1-x)^2}{x} \ln(1-x) - 6 + x \right], \quad (6)$$

where $\delta = \frac{3}{4}\beta + \frac{\alpha}{\pi}(\frac{\pi^2}{3} - \frac{1}{2}) + \beta^2(\frac{9}{32} - \frac{\pi^2}{12})$ and $\beta = \frac{2\alpha}{\pi}(\ln \frac{s}{m_e^2} - 1)$. A least χ^2 fit to the measured cross sections versus \sqrt{s} is performed with three free parameters f , ϕ , and $\mathcal{B}(\psi(2S) \rightarrow \gamma\pi^0)$. The χ^2 is defined as

$$\chi^2 = \sum_i \frac{(\sigma_i^{\text{obs}} - \sigma^{\text{exp}}(\sqrt{s}_i))^2}{(\Delta\sigma_i^{\text{obs}})^2 + \left(\Delta\sqrt{s}_i \cdot \frac{d\sigma^{\text{exp}}(\sqrt{s}_i)}{d\sqrt{s}} + \frac{1}{2}(\Delta\sqrt{s}_i)^2 \cdot \frac{d^2\sigma^{\text{exp}}(\sqrt{s}_i)}{d\sqrt{s}^2} \right)^2}, \quad (7)$$

where i denotes the i^{th} energy point and $\Delta\sigma^{\text{obs}}$ is the combination of statistical and uncorrelated systematic uncertainties. The second term in denominator estimates the uncertainty in the cross section due to the uncertainty of the c.m. energy [34].

Two optimal solutions are found as the consequence of the form of the fit formula as shown in Fig. 4 [35]. Table II shows detailed information about the two solutions. The uncertainties of the two solutions are not presented

where $\Delta = 1.3$ MeV is the c.m. energy spread and $F(x, s)$ is the radiator function, which is calculated with an accuracy of 0.1% and approximated as [33]

because the phase between $\psi(2S)$ and continuum amplitudes can not be determined due to the low statistics of the off-resonance data. We perform a two-dimensional parameters scan of ϕ and $\mathcal{B}(\psi(2S) \rightarrow \gamma\pi^0)$ to present the confidence interval of the fit result. Figure 5 shows the scanning result, where the value in each bin is the minimum χ^2 of the fit with ϕ and $\mathcal{B}(\psi(2S) \rightarrow \gamma\pi^0)$ fixed and f free. The steps of ϕ and $\mathcal{B}(\psi(2S) \rightarrow \gamma\pi^0)$ are 0.05 rad and 0.1×10^{-7} , respectively. The contours of $\pm 0.5\sigma$, $\pm 1\sigma$, $\pm 2\sigma$, and $\pm 3\sigma$ are corresponding to the value of $\chi_{\text{min}}^2 + 0.25$, $\chi_{\text{min}}^2 + 1$, $\chi_{\text{min}}^2 + 4$, and $\chi_{\text{min}}^2 + 9$, respectively. The 1σ contour is defined as the standard deviation of parameters approximately corresponding to the probability 39.3%. The 1σ contour range of $\mathcal{B}(\psi(2S) \rightarrow \gamma\pi^0)$ is $[2.7, 9.7] \times 10^{-7}$. The fit result of the form factor $f = |Q^2 F_{\pi^0}(Q^2)|$ is (0.215 ± 0.015) GeV in this energy region, where the uncertainty is the combination of sta-

tistical and uncorrelated systematic uncertainties.

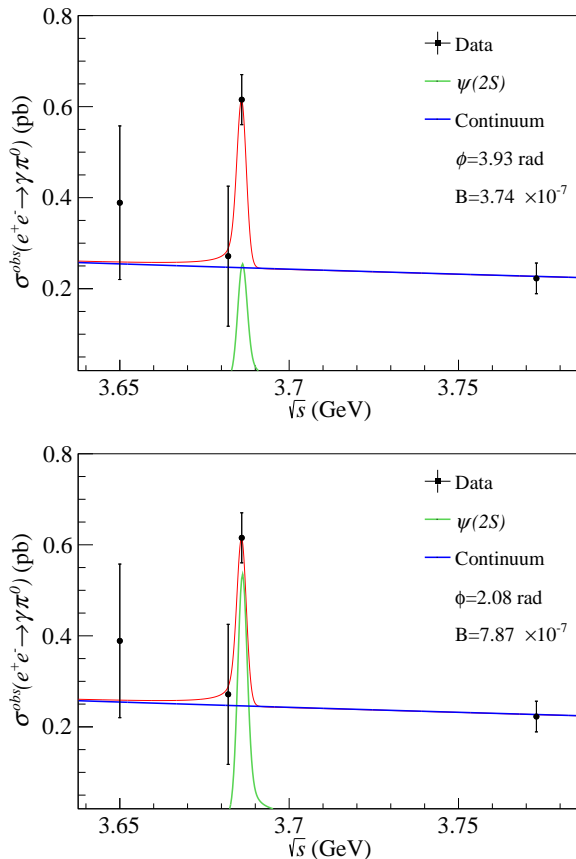


FIG. 4. Two optimal solutions of the fit to the observed cross section of $e^+e^- \rightarrow \gamma\pi^0$ in the vicinity of $\psi(2S)$ peak. Dots with error bars represent data, red solid lines denote fit results, green lines represent the contribution of $\psi(2S)$, blue lines represent the continuum contribution. Top panel is for solution a: $\mathcal{B}(\psi(2S) \rightarrow \gamma\pi^0) = 3.74 \times 10^{-7}$, $\phi = 3.93$ rad, and bottom panel is for solution b: $\mathcal{B}(\psi(2S) \rightarrow \gamma\pi^0) = 7.87 \times 10^{-7}$, $\phi = 2.08$ rad.

TABLE II. The information of two solutions.

	χ^2	$\mathcal{B}(\psi(2S) \rightarrow \gamma\pi^0)$	ϕ (rad)	f (GeV)
solution a	0.611	3.74×10^{-7}	3.93	0.215
solution b	0.611	7.87×10^{-7}	2.08	0.215

V. SYSTEMATIC UNCERTAINTY

Systematic uncertainties for the observed cross section include uncertainties from many sources, such as the integrated luminosity measurements, photon reconstruction efficiency, π^0 branching fraction, 4C kinematic fit, requirements on MDC hits, requirements on the number of photons, signal shape, and background shape. Each of these uncertainties is discussed in detail below:

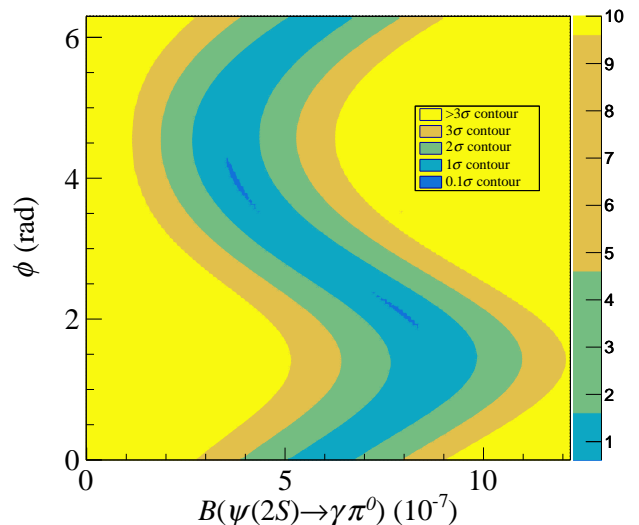


FIG. 5. The two-dimensional scanning result of ϕ and $\mathcal{B}(\psi(2S) \rightarrow \gamma\pi^0)$. The color represents the value of χ^2 .

A. Integrated luminosity

The uncertainties of the integrated luminosity measurement are studied using $e^+e^- \rightarrow \ell^+\ell^-(\gamma\gamma)$ ($\ell = e, \mu$) events with an uncertainty less than 1% [11–13]. We conservatively take 1% as the corresponding systematic uncertainty.

B. Photon detection efficiency

The uncertainty for photon detection is 0.5% per photon within barrel EMC region by studying $J/\psi \rightarrow \rho^0\pi^0$ process [36] and total uncertainty is 1.5%.

C. π^0 branching fraction

The uncertainty of the branching fraction of $\pi^0 \rightarrow \gamma\gamma$ in PDG [10] is considered as systematic uncertainty which is 0.03%.

D. 4C kinematic fit

The uncertainty of kinematic fit is studied by using a control sample $e^+e^- \rightarrow \gamma\gamma\gamma$ and the difference of the efficiency between the MC simulation and data is taken as the systematic uncertainty which is determined to be 1.0% [6].

E. Requirement on MDC hits

Based on the control sample $\psi(2S) \rightarrow \gamma\chi_{c2}$ with $\chi_{c2} \rightarrow \gamma\gamma$ which has same final state as the signal process. The

corresponding region used to count the number of hits in the MDC in this control sample is larger than that in the $\psi(2S) \rightarrow \gamma\pi^0$ decay due to the smaller Lorentz boost of the $\gamma\gamma$ system, and as a consequence, more hits from noise in the MDC will be counted in the control sample. To minimize this effect, the MDC hits are normalized according to area by assuming the noise is distributed uniformly over the MDC. The difference of the efficiency between data and MC simulation is determined to be 1.0% [6].

F. Requirement on the number of photons

The efficiency of the requirement on the number of photons is also studied with the control sample $\psi(2S) \rightarrow \gamma\chi_{c2}$ with $\chi_{c2} \rightarrow \gamma\gamma$. The data-MC difference is regarded as the systematic uncertainty which is 3.1% [6].

G. Signal shape

In the extraction of the number of signal events, the signal is described by a MC-simulated shape convolved with a Gaussian function with the mean and standard deviation as free parameters. However, for the fit on samples at $\sqrt{s} = 3.650$ and 3.682 GeV, the parameters of the Gaussian function are fixed due to low statistics at these energies. We change the values of the parameters of Gaussian function by one standard deviation from the fit at $\sqrt{s} = 3.686$ GeV and the differences are estimated as the systematic uncertainty. The results of uncertainties are 3.1% and 2.4% at $\sqrt{s} = 3.650$ and 3.682 GeV, respectively.

H. Background shape

In the fit to $\psi(2S)$ sample, the size of peaking backgrounds contribution from $\psi(2S) \rightarrow \gamma\chi_{cJ}$ decays with $\chi_{cJ} \rightarrow \pi^0\pi^0$ are fixed. We change the expected number of $\gamma\chi_{cJ}$ by ± 1 standard deviation in the fit and the largest difference is taken as the systematic uncertainty, which is 2.4%.

To study the uncertainty associated with smooth background shape, the background shape is changed from a third-order Chebychev function to a fourth-order Chebychev function in the fit and the difference is considered as the systematic uncertainty. The uncertainties are 3.1%, 1.4%, 0.2%, and 1.6% at $\sqrt{s} = 3.650, 3.682, 3.686,$ and 3.773 GeV, respectively.

I. Summary of the Systematic Uncertainty

All of the sources of the systematic uncertainties are listed in Table III. The systematic uncertainties of the cross section measurements are divided into correlated

and uncorrelated uncertainties. The correlated uncertainties are common to all energies including branching fraction of $\pi^0 \rightarrow \gamma\gamma$, the kinematic fit, the requirement on the number of photons, and the requirement on the number of MDC hits. The uncorrelated uncertainties are different at each energy including the signal shape, the background shape. The total uncertainty is calculated by

$$\sigma = \sqrt{\sum_i \sigma_i^2}, \quad (8)$$

where i denotes the i^{th} source of uncertainties assuming there is no correlation among them.

VI. SUMMARY

Based on $\psi(2S)$, $\psi(3770)$, and off-resonance data samples collected at 3.650 and 3.682 GeV, we measure the branching fraction of $\psi(2S) \rightarrow \gamma\pi^0$ and the form factor of $e^+e^- \rightarrow \gamma\pi^0$ at $-Q^2 \sim 13$ GeV². In the fit with the interference between $\psi(2S)$ and continuum amplitudes, two optimal solutions are found: $\mathcal{B}(\psi(2S) \rightarrow \gamma\pi^0) = 3.74 \times 10^{-7}$, $\phi = 3.93$ rad and $\mathcal{B}(\psi(2S) \rightarrow \gamma\pi^0) = 7.87 \times 10^{-7}$, $\phi = 2.08$ rad. The allowed range of $\mathcal{B}(\psi(2S) \rightarrow \gamma\pi^0)$ is $[2.7, 9.7] \times 10^{-7}$ with 1σ contour of χ^2 value. Comparing to the previous BESIII measurement of $\mathcal{B}(\psi(2S) \rightarrow \gamma\pi^0) = (9.5 \pm 1.7) \times 10^{-7}$ [6], the branching fraction tends to be smaller due to interference effects, consistent with the VMD prediction [7] within uncertainties. The contribution from continuum process $e^+e^- \rightarrow \gamma^* \rightarrow \gamma\pi^0$ is important and non-negligible in the measurement of $\mathcal{B}(\psi(2S) \rightarrow \gamma\pi^0)$. This measurement supports the VMD model's description of the vector charmonium radiative decays to light pseudoscalars.

In the framework of pQCD, the form factor is calculated as

$$\begin{aligned} |Q^2 F_{\pi^0}(Q^2)| &= \sqrt{2} f_{\pi^0} \left(1 - \frac{5}{3} \frac{\alpha_s(Q^2)}{\pi} \right) \\ &= \sqrt{2} f_{\pi^0} \approx 0.185 \text{ GeV at } Q^2 \rightarrow \infty, \end{aligned} \quad (9)$$

In this measurement, $f = |Q^2 F_{\pi^0}(Q^2)| = (0.215 \pm 0.015 \pm 0.004)$ GeV at $-Q^2 \sim 13$ GeV², where the first uncertainty is the combination of statistical and uncorrelated systematic uncertainties, the second uncertainty is correlated systematic uncertainty, and the total uncertainty is 0.016 GeV. This result is slightly larger than the pQCD value but agrees with it within 1.9σ deviation.

BaBar has suggested a parametrization of the form factor with the form

$$|Q^2 F_{\pi^0}(Q^2)| = A \left(\frac{Q^2}{10 \text{ GeV}^2} \right)^b, \quad (10)$$

where A and b are free parameters [37]. To compare our results with those of BaBar and Belle experiments,

TABLE III. Summary of systematic uncertainties (%) in the measurement of the $e^+e^- \rightarrow \gamma\pi^0$ cross section.

Sources	3.650 GeV	3.682 GeV	3.686 GeV	3.773 GeV
Photon reconstruction efficiency	1.5	1.5	1.5	1.5
$\mathcal{B}(\pi^0 \rightarrow \gamma\gamma)$	0.03	0.03	0.03	0.03
Requirement on N_γ	3.1	3.1	3.1	3.1
Kinematic fit	2.0	2.0	2.0	2.0
Number of MDC hits	1.0	1.0	1.0	1.0
Integrated luminosity	1.0	1.0	1.0	1.0
Signal shape	3.1	2.4	-	-
Peaking background	-	-	2.4	-
Smooth background shape	3.1	1.4	0.2	1.6
Total	6.1	5.1	4.9	4.5

the form factors at $|Q^2| = 3.686^2 \text{ GeV}^2$ from BaBar and Belle under this parametrization are calculated as $|Q^2 F_{\pi^0}(Q^2)| = 0.179 \pm 0.017$ and $0.197 \pm 0.008 \text{ GeV}$, respectively [38]. Belle has presented another parametrization defined as [38]

$$|Q^2 F_{\pi^0}(Q^2)| = \frac{BQ^2}{Q^2 + C}, \quad (11)$$

where B and C are free parameters, and corresponding value $|Q^2 F_{\pi^0}(Q^2)| = 0.180 \pm 0.017 \text{ GeV}$ at $Q^2 = 3.686^2 \text{ GeV}^2$. Comparison of these results for $|Q^2 F_{\pi^0}(Q^2)|$ between this work and other experiments is shown in Fig. 6, where the differences between our result with Belle and BaBar are 1.5σ and 1.0σ , respectively. The average of the three results are $|Q^2 F_{\pi^0}(Q^2)| = 0.197 \pm 0.007 \text{ GeV}$ when $|Q^2| = m^2(\psi(2S)) = 3.686^2 \text{ GeV}^2$.

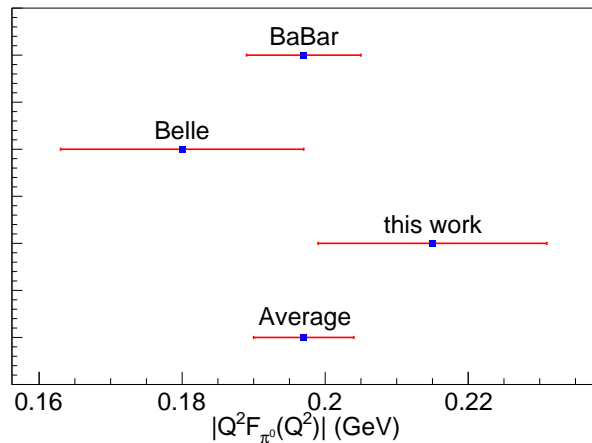


FIG. 6. $|Q^2 F_{\pi^0}(Q^2)|$ from different measurements at $|Q^2| = m^2(\psi(2S)) = 3.686^2 \text{ GeV}^2$.

ACKNOWLEDGMENTS

The BESIII Collaboration thanks the staff of BEPCII and the IHEP computing center for their strong support. This work is supported in part by National Key R&D Program of China under Contracts Nos. 2020YFA0406300, 2020YFA0406400, 2023YFA1606000; National Natural Science Foundation of China (NSFC) under Contracts Nos. 11635010, 11735014, 11935015, 11935016, 11935018, 12025502, 12035009, 12035013, 12061131003, 12192260, 12192261, 12192262, 12192263, 12192264, 12192265, 12221005, 12225509, 12235017, 12361141819; the Chinese Academy of Sciences (CAS) Large-Scale Scientific Facility Program; the CAS Center for Excellence in Particle Physics (CCEPP); Joint Large-Scale Scientific Facility Funds of the NSFC and CAS under Contract No. U1832207; 100 Talents Program of

CAS; The Institute of Nuclear and Particle Physics (IN-PAC) and Shanghai Key Laboratory for Particle Physics and Cosmology; German Research Foundation DFG under Contracts Nos. 455635585, FOR5327, GRK 2149; Istituto Nazionale di Fisica Nucleare, Italy; Ministry of Development of Turkey under Contract No. DPT2006K-120470; National Research Foundation of Korea under Contract No. NRF-2022R1A2C1092335; National Science and Technology fund of Mongolia; National Science Research and Innovation Fund (NSRF) via the Program Management Unit for Human Resources & Institutional Development, Research and Innovation of Thailand under Contract No. B16F640076; Polish National Science Centre under Contract No. 2019/35/O/ST2/02907; The Swedish Research Council; U. S. Department of Energy under Contract No. DE-FG02-05ER41374

-
- [1] N. Morisita, I. Kitamura, and T. Teshima, *Phys. Rev. D* **44**, 175 (1991).
- [2] H. Fritzsche and J. D. Jackson, *Phys. Lett. B* **66**, 365 (1977).
- [3] K. T. Chao, *Nucl. Phys. B* **335**, 101 (1990).
- [4] V. L. Chernyak and A. R. Zhitnitsky, *Phys. Rept.* **112**, 173 (1984).
- [5] G. W. Intemann, *Phys. Rev. D* **27**, 2755 (1983).
- [6] M. Ablikim *et al.* (BESIII Collaboration), *Phys. Rev. D* **96**, 052003 (2017), arXiv:1708.03103 [hep-ex].
- [7] Q. Zhao, *Phys. Lett. B* **697**, 52 (2011), arXiv:1012.1165 [hep-ph].
- [8] G. P. Lepage and S. J. Brodsky, *Phys. Rev. D* **22**, 2157 (1980).
- [9] E. Braaten, *Phys. Rev. D* **28**, 524 (1983).
- [10] R. L. Workman *et al.* (Particle Data Group), *PTEP* **2022**, 083C01 (2022).
- [11] M. Ablikim *et al.* (BESIII Collaboration), *Chin. Phys. C* **48**, 093001 (2024), arXiv:2403.06766 [hep-ex].
- [12] M. Ablikim *et al.* (BESIII Collaboration), *Phys. Lett. B* **753**, 629 (2016), [Erratum: *Phys.Lett.B* 812, 135982 (2021)], arXiv:1507.08188 [hep-ex].
- [13] M. Ablikim *et al.* (BESIII Collaboration), (2024), arXiv:2406.05827 [hep-ex].
- [14] M. Ablikim *et al.* (BESIII Collaboration), *Nucl. Instrum. Meth. A* **614**, 345 (2010), arXiv:0911.4960 [physics.ins-det].
- [15] C. Yu *et al.*, in *7th International Particle Accelerator Conference* (2016) p. TUYA01.
- [16] M. Ablikim *et al.* (BESIII Collaboration), *Chin. Phys. C* **44**, 040001 (2020), arXiv:1912.05983 [hep-ex].
- [17] J. Lu, Y. Xiao, and X. Ji, *Radiat. Detect. Technol. Methods* **4**, 337 (2020).
- [18] J. W. Zhang *et al.*, *Radiat. Detect. Technol. Methods* **6**, 289 (2022).
- [19] X. Li *et al.*, *Radiat. Detect. Technol. Methods* **1**, 13 (2017).
- [20] Y. X. Guo *et al.*, *Radiat. Detect. Technol. Methods* **1**, 15 (2017).
- [21] P. Cao *et al.*, *Nucl. Instrum. Meth. A* **953**, 163053 (2020).
- [22] S. Agostinelli *et al.* (GEANT4), *Nucl. Instrum. Meth. A* **506**, 250 (2003).
- [23] S. Jadach, B. F. L. Ward, and Z. Was, *Phys. Rev. D* **63**, 113009 (2001), arXiv:hep-ph/0006359.
- [24] S. Jadach, B. F. L. Ward, and Z. Was, *Comput. Phys. Commun.* **130**, 260 (2000), arXiv:hep-ph/9912214.
- [25] D. J. Lange, *Nucl. Instrum. Meth. A* **462**, 152 (2001).
- [26] R.-G. Ping, *Chin. Phys. C* **32**, 599 (2008).
- [27] J. C. Chen, G. S. Huang, X. R. Qi, D. H. Zhang, and Y. S. Zhu, *Phys. Rev. D* **62**, 034003 (2000).
- [28] R.-L. Yang, R.-G. Ping, and H. Chen, *Chin. Phys. Lett.* **31**, 061301 (2014).
- [29] E. Richter-Was, *Phys. Lett. B* **303**, 163 (1993).
- [30] M. Ablikim *et al.* (BESIII Collaboration), *Phys. Rev. Lett.* **105**, 261801 (2010), arXiv:1011.0885 [hep-ex].
- [31] W. Sun, T. Liu, M. Jing, L. Wang, B. Zhong, and W. Song, *Front. Phys. (Beijing)* **16**, 64501 (2021), arXiv:2011.07889 [hep-ex].
- [32] J. P. Alexander, G. Bonvicini, P. S. Drell, R. Frey, and V. Luth, *Nucl. Phys. B* **320**, 45 (1989).
- [33] E. A. Kuraev and V. S. Fadin, *Sov. J. Nucl. Phys.* **41**, 466 (1985).
- [34] B. P. Roe, *Probability and Statistics in Experimental Physics* (Springer New York, NY).
- [35] K. Zhu, X. H. Mo, C. Z. Yuan, and P. Wang, *Int. J. Mod. Phys. A* **26**, 4511 (2011), arXiv:1108.2760 [hep-ex].
- [36] M. Ablikim *et al.* (BESIII Collaboration), *Phys. Rev. Lett.* **116**, 251802 (2016), arXiv:1603.04936 [hep-ex].
- [37] B. Aubert *et al.* (BaBar Collaboration), *Phys. Rev. D* **80**, 052002 (2009), arXiv:0905.4778 [hep-ex].
- [38] S. Uehara *et al.* (Belle Collaboration), *Phys. Rev. D* **86**, 092007 (2012), arXiv:1205.3249 [hep-ex].